UNIVERSITY OF LEEDS

Article:
Nakatani, Y, Shimaki, Y, Debajyoti, D et al. (4 more authors) (2020) Unprecedented mode of action of phenothiazines as ionophores unravelled by an NDH-2 bioelectrochemical assay platform. Journal of the American Chemical Society, 142 (3). pp. 1311-1320. ISSN 0002-7863

https://doi.org/10.1021/jacs.9b10254

Unprecedented mode of action of phenothiazines as ionophores unravelled by an NDH-2 bioelectrochemical assay platform

Journal:	*Journal of the American Chemical Society*
Manuscript ID	ja-2019-10254c.R2
Manuscript Type:	Article
Date Submitted by the Author:	17-Dec-2019
Complete List of Authors:	Nakatani, Yoshio; University of Otago, Microbiology and Immunology Shimaki, Yosuke; University of Otago, Microbiology and Immunology Dutta, Debajyoti; University of Leeds, Faculty of Biological Sciences Muench, Stephen; University of Leeds, School of Biomedical Sciences Ireton, Keith; University of Otago, Microbiology and Immunology Cook, Gregory; University of Otago Jeuken, Lars; University of Leeds, School of Biomedical Sciences, the Astbu

Unprecedented properties of phenothiazines unraveled by a NDH-2 bioelectrochemical assay platform

Yoshio Nakatani[1,2]‡*, Yosuke Shimaki[1]‡, Debajyoti Dutta[3], Stephen P. Muench[3], Keith Ireton[1], Gregory M. Cook[1,2], Lars J. C. Jeuken[3]*

1. Department of Microbiology and Immunology, University of Otago, Dunedin 9054, New Zealand

2. Maurice Wilkins Centre for Molecular Biodiscovery, The University of Auckland, Private Bag 92019, Auckland 1042, New Zealand

3. School of Biomedical Sciences and the Astbury Centre for Structural Molecular Biology, University of Leeds, Leeds LS2 9JT, United Kingdom

‡These authors contributed equally.

*Authors for correspondence: Yoshio Nakatani (yoshio.nakatani@otago.ac.nz) and Lars J. C. Jeuken (L.J.C.Jeuken@leeds.ac.uk)

Abstract

Type II NADH:quinone oxidoreductase (NDH-2) plays a crucial role in the respiratory chains of many organisms. Its absence in mammalian cells makes NDH-2 an attractive new target for developing antimicrobials and anti-protozoal agents. We established a novel bioelectrochemical platform to characterize the catalytic behavior of NDH-2 from *Caldalkalibacillus thermarum* and *Listeria monocytogenes* strain EGD-e while bound to native-like lipid membranes. Catalysis of both NADH oxidation and lipophilic quinone reduction by membrane-bound NDH-2 followed the Michaelis–Menten model; however, the maximum turnover was only achieved when a high concentration of quinone (>3 mM) was present in the membrane, suggesting that quinone availability regulates NADH-coupled respiration activity. The quinone analogue 2-heptyl-4-hydroxyquinoline-*N*-oxide inhibited *C. thermarum* NDH-2 activity and its potency is higher in a membrane environment compared to assays performed with water-soluble quinone analogues, demonstrating the importance of testing compounds under physiologically relevant conditions. Furthermore, when phenothiazines, one of the most commonly identified NDH-2 inhibitors, were tested, they did not inhibit membrane-bound NDH-2. Instead, our assay platform unexpectedly suggests a novel mode of phenothiazine action where chlorpromazine, a promising anti-tubercular agent and key medicine used to treat psychotic disorders, is able to disrupt pH gradients across bacterial membranes.

Introduction

NADH dehydrogenase/NADH:quinone oxidoreductase (NDH) is a key respiratory enzyme in many organisms. This class of enzymes catalyzes oxidation of NADH and reduction of quinone, and plays a crucial role in maintaining the cellular NAD^+/NADH balance and serves as a primary electron entry point for the respiratory chain to drive ATP synthesis. Type II NADH:quinone oxidoreductase (NDH-2) is a 40–70 kDa single subunit monotopic membrane protein distinct from two other functionally related NDHs—the proton pumping type NDH (NDH-I/complex I) and the sodium pumping type NDH (NQR).[1,2] NDH-2 has two Rossmann fold domains linked to the non-conserved C-terminal membrane-anchoring domain.[3-6] Nucleotide binding domains are exposed to the cytosol and responsible for binding NADH and hosting flavin co-factors FAD/FMN, whereas the quinone-binding site (Q-site) is located at the C-terminal domain proposed to face the lipid membrane.[5-7] The FAD isoalloxazine is midway between the NADH binding site and Q-site, and is the catalytic center of NDH-2 where exergonic reactions of NADH oxidation and quinone reduction take place.[8] Because of its structural and catalytic simplicity, NDH-2 does not transfer protons across the membrane and does not directly contribute to generation of proton motive force.[8] This might be advantageous for some organisms in the maintenance of the NAD^+/NADH redox balance and generation of ATP because its catalytic function cannot be compromised by proton motive force back-pressure.

The *ndh-2* gene has been identified in a wide range of organisms ranging from bacteria, fungi, protists and plants but not in any mammals,[4] which makes it an attractive target for antimicrobial development. Iodonium derivatives,[9,10] flavones,[11,12] quinolones,[13-21] phenothiazines,[11,22,23] and nanaomycin A and polymyxin B[24,25] have been identified as NDH-2 inhibitors with moderate activities. Among them, quinolones and phenothiazines are the most commonly identified NDH-2 inhibitors for many species, and quinolones, represented by 2-heptyl-4-hydroxyquinoline-*N*-oxide (HQNO), have the best biochemical and structural validation.[26] Their quinolone bicyclic core structure mimics a menaquinone head group. In bacterial and yeast NDH-2 quinolone complex structures, the head groups of HQNO and AC0-12 bind next to the *si* face of the FAD prosthetic group at the Q-site, blocking quinone access.[26,27] Since the discovery of their anti-tubercular activities, phenothiazines have been regarded as promising compounds for development of new antimicrobials.[28] However, the molecular inhibition mechanism of phenothiazines remains unclear despite their inhibitory activity against many NDH-2s. After discovery of the *ndh-2* gene essentiality in survival of the

important pathogens *Mycobacterium tuberculosis*[29,30] and *Plasmodium falciparum*,[9,16] several major anti-tubercular and -malarial drug development programs have been pursued by academia and industry, and potent (low nanomolar inhibition activity) quinolone and quinolinyl pyrimidine derivatives have been developed through medicinal chemistry approaches.[14,15,31] However, to date, there has been little success in the development of drugs targeting NDH-2. One major impediment to rationale development of NDH-2 therapeutics is a lack of understanding of the inhibition mechanisms.

Knowledge of the molecular structure and catalytic mechanism of NDH-2 is essential for development of new therapeutics against NDH-2, but these have just started being uncovered despite over half a century of NDH-2 research. Early on, NDH-2 research relied on membrane extracts, which have little NDH-2 activity. Even after establishing heterologous over-expression systems for NDH-2, extracting and purifying highly active NDH-2s from membranes using detergents remains challenging. Screening compounds using membrane extracts or materials with low activity might result in failure to identify promising hits and improve the specificity of NDH-2 inhibitors. Until now, only six highly active NDH-2s (turnover rates (k_{cat}) in the range of 580–1500 s^{-1}) have been reported from *Saccharomyces cerevisiae*,[27] *Caldalkalibacillus thermarum*,[8] *Staphylococcus aureus*,[23] *Plasmodium falciparum*,[32] *Mycobacterium tuberculosis*,[33] and *Streptococcus agalactiae*.[34] Importantly, crystal structures for all these NDH-2s, except those from *M. tuberculosis* and *S. agalactiae*, have been determined.[5,6,13,32] The use of highly stable and active NDH-2 has allowed us to unambiguously unravel its catalytic mechanism.[8]

We have previously developed a bioelectrochemical system coupled with a tethered bilayer lipid membrane to study respiratory enzyme behavior in a native-like environment.[35,36] This sensitive analytical method can detect catalytic activity in membrane extracts or purified respiratory enzymes.[35,37,38] Such a system is ideal to characterize "difficult membrane proteins" like NDH-2. Here, we developed a novel NDH-2 bioelectrochemical platform (Figure 1A) and analyzed catalysis of the membrane-bound *C. thermarum* NDH-2. Validation of NDH-2 inhibitors and elucidation of their modes of action in membranes uncovered some unexpected behaviors of phenothiazines. Furthermore, we adapted our bioelectrochemical platform to study NDH-2 from *Listeria monocytogenes*, showing its superiority over conventional biochemical assays that requires a very small amount of NDH-2 for kinetic characterization and inhibitor tests.

Results and Discussion

Establishing a new NDH-2 bioelectrochemical assay platform

Impedance spectroscopy confirmed that planar membranes containing *C. thermarum* NDH-2 spontaneously formed after applying a solution of *Escherichia coli* polar lipid proteoliposomes, pre-mixed with purified *C. thermarum* NDH-2, onto an electrode with a self-assembled monolayer containing cholesterol "tethers" (Figure 1B).[35] The E. coli polar lipids were supplemented by menaquinone-7 (MK-7). Cyclic voltammetry (CV) was used to characterize kinetics by monitoring quinone reduction activity, which is directly visible as catalytic currents. Figure 2A (blue trace) shows a CV in the absence of NADH where a MK-7 oxidation peak is visible at ~0.15 V versus standard hydrogen electrode (SHE) and the corresponding reduction peak at ~–0.3 V. Small UQ-8 reduction and oxidation signals are also visible at approximately –0.1 and 0.35 V, respectively. UQ-8 is naturally present in the *E. coli* lipid extract used to make the membrane-coated electrodes.[35] Addition of NADH produced a sigmoidal CV trace with the same onset as MK-7 oxidation, confirming NADH:MK-7 oxidoreduction activity. Activity of the membrane-bound *C. thermarum* NDH-2 followed a Michaelis–Menten model (Figures 2A–C and S1A), consistent with our reported in-solution assay results.[8] We did not observe unusual catalytic behaviors such as an allosteric mechanism as proposed for *P. falciparum* NDH-2[32] or the two quinone-binding model that was proposed by Godoy-Hernandez *et al*. (which was reported during the peer-review process of this article).[39] The estimated K_M^{NADH} of 8.6 μM was slightly lower than but comparable to the K_M^{NADH} of the in-solution assay (29 μM). By contrast, the $K_M^{MK\text{-}7}$ was two orders of magnitudes higher (3.2 mM) than that of the in-solution assay ($K_M^{Menadione}$ = 34 μM). We previously observed similar behavior of the $K_M^{Ubiquinone\text{-}10}$ of a ubiquinol oxidase.[37] The high $K_M^{MK\text{-}7}$ suggests that lipophilic quinone transfer between the NDH-2 Q-site and the quinone-pool in the membrane environment is slow and the quinone concentration can become a rate-limiting step. The maximum turnover rate was approximately 1.9–2.0 μA cm^{-2} (Figures 2B and 2C). Based on the protein-to-lipid ratio used, we estimate a surface coverage of *C. thermarum* NDH-2 in the order of 20-40 fmol cm^{-2}, resulting in an estimated k_{cat} (250–600 s^{-1}) at 20°C, slightly lower than the in-solution k_{cat} which was measured at the higher temperature of at 37°C (1190 s^{-1}) in the previous study.[8] NADPH titration confirmed the low binding affinity of NADPH (K_M^{NADPH} of 367.4 μM, Figures 2D and S1B), which was consistent with a previous result.[8] The maximum turnover rate was lower (1.4 μA cm^{-2}). After washing the electrochemical cell, addition of NADH restored the rate close to

2.0 μA cm^{-2} (Figures 2D, S1B and S1C). This example highlights the reproducibility and versatility of our NDH-2 electrochemical platform.

To further validate our system, we tested nucleotide-binding and Q-site mutants.[8] G164E and I379E NDH-2 variants have ablated binding ability to either NADH or the water-soluble quinone menadione (MD), respectively.[8] Figures 2E and 2F show drastic reductions in the turnover rates for both mutants. G164E and I379E NDH-2 variants showed only 2.8% and 6.3% of wild-type activity (at 200 μM NADH), respectively (Figures 2E, 2F, S1D and S1E). The K_M^{NADH} of the G164E mutant could not be determined but the calculated K_M^{NADH} of the Q-site mutant (I379E) was 1.3 μM. This lower K_M^{NADH} compared to the wild-type most likely represents the capping effect observed in the previous study.[8] Notably, the Q-site mutant showed a greater reduction in activity in the membrane (94% reduction, compare Figure 2F to Figure 2B) than in solution (~50%).[8] This suggests that the I379E mutation is structurally more significant in a membrane environment and causes more adverse effects against lipophilic quinone binding.

Evaluating NDH-2 inhibitors using the new NDH-2 bioelectrochemical assay platform

Proposed NDH-2 inhibitors, including HQNO and three phenothiazines (chlorpromazine (CPZ), trifluoperazine (TPZ), and thioridazine (THZ), Figure 3A) were tested against *C. thermarum* NDH-2. HQNO inhibited *C. thermarum* NDH-2 with an IC_{50} of 6.8 μM (Figures 3B and 3C), similar to that for the in-solution assay (7.3 μM).[26] This was somewhat surprising since a large excess of quinone is present in the membrane (> 3–7 mM), compared with MD in the in-solution assay (50 μM).[26] This suggests that the HQNO binding affinity to *C. thermarum* NDH-2 in the membrane greatly increases and efficiently blocks quinone access to the Q-site. Washing the cell restored activity to ~50%, which suggested that HQNO remains in the membrane causing NDH-2 inhibition (Figure S2A). Interestingly, we discovered that phenothiazines were largely ineffective at inhibiting *C. thermarum* NDH-2 (Figures 3D, 3E, S2B and S2C). These results were unexpected given that TPZ and THZ inhibited detergent-purified *C. thermarum* NDH-2 in the presence of Coenzyme Q2 (ubiquinone-2, UQ-2) in a previous study.[6] Therefore, we performed additional in-solution assays and electrochemical experiments, which confirmed that phenothiazines were largely ineffective against NDH-2. First, TPZ and THZ did not show significant inhibition when measuring activity in solution with MD (Figure S2D). Second, our electrochemical assay confirmed CPZ also did not inhibit

membrane-bound *C. thermarum* NDH-2 in the presence of ubiquinone-10 (Figures S2E and S2F). It is unclear why TPZ and THZ previously inhibited *C. thermarum* NDH-2 activity in the presence of UQ-2; however, we propose that the membrane environment in the electrochemical platform better represents the natural physiological environment of NDH-2 than the solution/UQ-2 assay used previously.

Although there was very little NDH-2 inhibition by phenothiazines, we noticed that these compounds caused the catalytic waves to shift to different degrees (Figures 3D, S2B and S2C). Without NADH, shifts of MK-7 oxidation and reduction peaks were also clearly observed (Figure 4A). Furthermore, redox peaks of a minor fraction of UQ-8 shift to similar degree (Figure 4A). Importantly, the potential difference between the quinone oxidation and reduction peaks decreased. We previously observed a very similar effect when a protonophore, carbonyl cyanide *m*-chlorophenyl hydrazone (CCCP) was added to the membrane-modified electrodes and this was shown to be caused by an enhancement in proton mobility through the membrane which aids the (de)protonation of the lipophilic quinones that is coupled to their oxidation/reduction.[38] Taken together these observations suggest CPZ acts as a protonophore. Impedance spectroscopy was performed to confirm this hypothesis. Indeed, in the Bode plot (Figure 4B) a large drop in phase is observed below 10 Hz upon addition of CPZ, which is characteristic of reduction in membrane resistance (increase in membrane permeability) and thus consistent with an ionophore effect.[35,40] Additionally, we performed solution assays with liposomes encapsulating 8-hydroxypyrene-1,3,6-trisulfonic acid (HPTS) as a fluorescent pH probe. After changing the pH on the outside of the liposomes, protons were observed to leak into the liposomes and slowly equilibrated (Figure 4C). As expected, further addition of gramicidin, a powerful ionophore, resulted in immediate pH equilibration. By contrast, adding CPZ caused a large increase in the lumen pH, followed by faster pH re-equilibration. We speculated this is caused by the tertiary amine of CPZ, which has a pKa of 9.3. CPZ would initially crosses the membrane in a neutral form (non-protonated) and then picks up a proton in the lumen of the liposome, rapidly increasing the pH. Then, in a slower process, CPZ seems to act as a protonophore, increasing the rate of pH equilibration. The protonophore activity could be attributed to the fact that CPZ-H^+ is still able to traverse the membrane, although at a much slower rate than CPZ. These unexpected findings in CPZ chemical properties might have implications in other biological membrane systems. CPZ is a key medicine in the World Health Organization Model List of Essential Medicines and is used to treat psychotic disorders.[41] CPZ affects a number of receptors in the human nervous system, including dopamine, serotonin,

histamine, adrenergic, and muscarinic acetylcholine receptors, but its molecular effects on the nervous system remain largely unknown.[42] Further testing of CPZ is of interest to see if it shows a similar effect against mammalian membranes and the human nervous system.

Characterization of *Listeria monocytogenes* EGD-e NDH-2a using a bioelectrochemical NDH-2 assay platform.

Next, we adapted our bioelectrochemical NDH-2 system to characterize a *Listeria* NDH-2 enzyme. A foodborne pathogen, *Listeria monocytogenes* strain EGD-e possesses two *ndh-2* genes (*lmo2389* and *2638* designated as *ndh-2a* and *-2b*, respectively). Because NDH-2a is an important enzyme for aerobic and intracellular growth of *L. monocytogenes*,[43] we prioritized characterization of NDH-2a. Despite high amino acid sequence similarity to *C. thermarum* NDH-2 (54% and 72% identity and similarity, respectively; Figure S3A), detergent-purified *Listeria* NDH-2a was unstable and difficult to purify. Thus, we used styrene maleic anhydride (SMA) polymer[44] to purify *Listeria* NDH-2a (Figure S3B) with ~150 μg of SMA-purified NDH-2a obtained from a 3-L culture. However, because only a small proportion (< 5%) of the purified sample contained FAD (UV-Vis analysis), conventional biochemical characterization was not possible. We used SMA-purified *Listeria* NDH-2a to create proteoliposomes and applied these to the self-assembled monolayer-coated gold electrode. Impedance spectroscopy again confirmed that the membrane-coated electrode formed immediately (Figure 5A). The estimated K_M^{NADH} of *Listeria* NDH-2a is 14.8 μM and comparable to that of *C. thermarum* NDH-2 and to the reported K_M^{NADH}s of NDH-2 from other species (Figures 5B and 5C).[5,8,13,32-34] The maximum turnover rate was approximately 40% of that of *C. thermarum* NDH-2. Given the use of SMA-solubilized *Listeria* NDH-2, the estimation of the lipid-to-protein ratio in the proteoliposomes less certain, further experiments will be required to determine k_{cat} (s^{-1}). Immediately after NADH titration, we performed HQNO titration experiments using the same cell. Interestingly, HQNO showed weaker inhibition against *Listeria* NDH-2a than against *C. thermarum* NDH-2, with a maximum inhibition activity of approximately 38% (Figures 5D and S3C). The membrane anchoring domain of NDH-2 is the least conserved among the species (Figures S3A, S3D and S3E). Critically, two amino acids in the quinone-head group binding pockets differ between *Listeria* and *C. thermarum* NDH-2s (I320M and Y383A, amino acid numbers from *C. thermarum* NDH-2), which could alter its structural architecture and impact the HQNO binding affinity (Figure S3F). Together with observation that a I379E mutation of *C. thermarum* NDH-2 has a more pronounced effect in the electrochemical

membrane platform (see above), a membrane environment seems to accentuate effects of amino acid substitutions at the Q-site compared to in-solution. Furthermore and seen the dissimilarities of NDH-2 across different species, these results indicate that the developed new antimicrobials or anti-protozoal agents targeting NDH-2 might be narrow-spectrum.

Conclusion

In summary, we built a novel bioelectrochemical platform to characterize the monotopic respiratory enzyme NDH-2 in a native-like lipid environment. This system has four major advantages over the conventional biochemical assay: (1) it allows both characterization of NDH-2 and assessment of inhibitors in close to physiological conditions (i.e., in-membrane), (2) it requires only a very small amount (< 0.45 pg) of active NDH-2, (3) it is versatile as shown by performance of inhibitor experiments after NADH titration and reuse of the electrochemical cell, and (4) the chemical properties of inhibitors in the membrane can be analyzed. Furthermore, our system is highly reproducible and stable for > 12 h with no reduction in activity.

Two NDH-2s from *C. thermarum* and *L. monocytogenes* EGD-e were successfully characterized. The membrane-bound NDH-2 follows Michaelis–Menten kinetics for both NADH and MK-7. Interestingly, we discovered that NDH-2 required a high quinone concentration (> 3 mM) to reach its full catalytic performance. This might imply the quinone concentration in the membrane is biologically important, and that the NADH-coupled respiratory activity in bacteria might be regulated by quinone availability in the membrane.

Unexpectedly, we discovered that a class of promising anti-tubercular agents, phenothiazines, have novel effects. Cyclic voltammetry and impedance spectroscopy of the bioelectrochemical platform, together with solution assays with liposomes encapsulating HPTS, indicate that CPZ can disrupt pH gradients across bacterial membranes.

Materials and Methods

Chemicals

Escherichia coli polar phospholipid extract in chloroform (Avanti), menaquinone-7 (FUJIFILM Wako), Ni-NTA Agarose Resin (Thermo Fisher Scientific), 8%–16% Mini-PROTEAN TGX precast gels (Bio-Rad), and 2-heptyl-4-hydroxyquinoline-*N*-oxide (Santa Cruz Biotech) were purchased for use in this study. Chlorpromazine, trifluoperazine,

thioridazine, 6-mercapto-1-hexanol (99%), ubiquinone-10 and 8-hydroxypyrene-1,3,6-trisulfonic acid were purchased from Sigma–Aldrich. The styrene maleic anhydride polymer XIRAN SL30010 P20 was kindly provided by Polyscope.

Caldalkalibacillus thermarum NDH-2 and *Listeria monocytogenes* EGD-e NDH-2a (*lmo2389*) expression constructs

In previous studies, we used a *C. thermarum* NDH-2 with a hexahistidine tag at its C-terminus for in-solution biochemical and biophysical studies.[6,8,26,45] However, this tag was linked immediately after two amphipathic α-helices that are anchored to the membrane,[6,45] which potentially compromised the binding ability of *C. thermarum* NDH-2 to the membrane. The N-terminus of *C. thermarum* NDH-2 is exposed to the cytosol and physically distant from the membrane interface. Therefore, we switched the hexahistidine tag to the N-terminus. PCR was performed as previously described except the primers N-Hisndh2F (5'-AAATTTCCATGGGCCACCATCACCATCACCATAGCAAACCAAGCATTGTG-3') and N-Hisndh2R (5'-AAATTTGTCGACTCAAAAACGCCCTTTTTTCAA-3') were used to amplify the *C. thermarum ndh-2* gene with an additional hexahistidine tag at its N-terminus.[6] The PCR product was cloned into pTRC99a as previously described.[6] G164E and I379E variants were also constructed similarly except templates constructed in previous work were used.[8]

To clone a *L. monocytogenes* EGD-e *ndh-2a* (*lmo2389*), PCR was performed using *L. monocytogenes* EGD-e genomic DNA as a template and a primer set of lmo2389-N-HisF (5'-AAAAAACCATGGGTCACCATCACCATCACCATAAACCAAAAATTGTCATTCTCG GAGCAG-3') and lmo2389-N-HisR (5'-AAAAAAGTCGACTCATTTATAGAATTTGAATTTACCTTTACTTGCCAAGACGC-3'). PCR mix containing Phusion™ DNA polymerase was prepared according to the manufacturer's recommendations (FINNZYMES). The initial denaturation step was for 5 min at 95 °C, followed by 35 cycles of amplification (30 s at 95 °C, 30 s at 55 °C, and 1 min at 72 °C). A final extension step was carried out at 72 °C for 10 min. PCR products of the *L. monocytogenes* EGD-e *ndh-2a* gene were digested using the restriction enzymes NcoI and SalI, and then cloned into pTRC99a. The resulting expression construct was named pTRC99a-N-His*ndh-2a*.

Expression and purification of *C. thermarum* NDH-2 and *L. monocytogenes* EGD-e NDH-2a

Caldalkalibacillus thermarum NDH-2 was expressed and purified as described previously.[6] In the size-exclusion purification step, similar concentrations of wild-type, G164E, and I379E NDH-2 variants were loaded on the column so that the fractions had similar protein concentrations. All variants were eluted from the column in a very similar manner. After the fractions were analyzed by SDS-PAGE, samples were pooled and concentrated. All variant samples had similar protein and detergent concentrations. Glycerol (10%, w/v) was added to the concentrated samples, and the samples (final protein concentration of 4 mg mL^{-1}) were flash-frozen in liquid nitrogen and stored at −80 °C. Of note, switching the tag did not affect the catalytic activity of NDH-2. The specific activity was measured as previously described in the presence of 200 μM NADH and 400 μM MD at 37 °C.[8,26] The activity of the N-terminally histidine-tagged *C. thermarum* wild-type NDH-2 was 980 s^{-1} and consistent with that measured for the C-terminally histidine-tagged *C. thermarum* wild-type NDH-2.[8,26]

For over-expression of *L. monocytogenes* EGD-e NDH-2a, *E. coli* C41 (DE3) cells[46] were transformed using a pTRC99a-N-His*ndh-2a* expression construct. To express *Listeria* NDH-2a, transformed *E. coli* were inoculated into 800 mL of LB media containing 100 μg mL^{-1} ampicillin and grown at 37° C and 200 rpm to reach an OD_{600} of approximately 0.6–0.7. After cooling the cell culture at 4 °C for 10 min, isopropyl-β-D-thiogalactopyranoside (final concentration of 0.5 mM) was added and the cell culture was incubated at 18 °C and 200 rpm. Approximately 1 day later, the OD_{600} of the cell culture reached 1.9–2.0. Cells were harvested by centrifugation and the cell pellets were stored at −80 °C.

To extract *E. coli* membrane containing over-expressed *Listeria* NDH-2a, 80 mL of lysis buffer (50 mM Tris pH 7.5 containing 2 mM $MgCl_2$) was added to the pellet obtained from the 1-L culture. The resuspended cells were French pressed twice at 10000 psi. The cell lysate was subjected to centrifugation at 8000 ×*g*, 4 °C for 15 min. The obtained supernatant was subjected to ultracentrifugation at 146000 ×*g*, 4°C for 1 h to isolate the *E. coli* membrane. The harvested membrane was flash-frozen in liquid nitrogen and stored at −80 °C.

To purify *Listeria* NDH-2a, a SMA polymer method was employed.[44] The membrane was resuspended in Buffer A (50 mM Tris buffer, pH 8.0, containing 500 mM NaCl and 10% (v/v)

glycerol) to give a final membrane concentration of 80 mg mL^{-1}. Then, 5% (w/v) SMA buffer (50 mM Tris buffer, pH 8.0, containing 500 mM NaCl, 10% (v/v) glycerol and 5% (w/v) XIRAN SL30010 P20) was added to give a final membrane concentration of 40 mg mL^{-1} and SMA (XIRAN SL30010 P20) content of 2.5% (w/v). The resulting sample was incubated at room temperature for 2 h with gentle agitation. The insoluble fraction was removed by centrifugation at 100000 ×*g*, 4 °C for 45 min. Ni-NTA resin equilibrated with Buffer A was added to the supernatant (1-mL resin bed volume to 1 g of membrane) and incubated at 4 °C overnight with gentle agitation. The sample was transferred to an Econo-Column (Bio-Rad) and the unbound fraction was collected. The resin was first washed with Buffer A and then washed with Buffer A containing 10 mM imidazole. The bound *Listeria* NDH-2a was eluted using Buffer A containing 300 mM imidazole. The fractions were analyzed by SDS-PAGE. The 300 mM imidazole fraction was buffer exchanged with 50 mM Tris buffer (pH 8.0, containing 150 mM NaCl) and the sample was concentrated to 3 mg mL^{-1}. Finally, the sample was flash-frozen in liquid nitrogen and stored at −80 °C.

Reconstitution of *C. thermarum* NDH-2 and *Listeria* NDH-2a in an *E. coli* polar lipid proteoliposome

An established extrusion protocol was used for proteoliposome reconstitution with a modification to use 200-nm nucleopore track-etched membrane (Whatman).[35] For reconstitution of *C. thermarum* NDH-2, 5 mg of *E. coli* polar lipid, 50 μg of MK-7/ubiquinone-10 (UQ-10), and 20 μg of purified *C. thermarum* NDH-2 were extruded into 1 mL of 20 mM MOPS–KOH buffer (pH 7.4, containing 30 mM K_2SO_4). For MK-7 titration experiments, 12.5, 25, 37.5, 50, or 75 μg of MK-7 was incorporated. For reconstitution of *Listeria* NDH-2a, 5 mM $MgCl_2$ (final concentration) was added to 60 μg of SMA purified *Listeria* NDH-2a and the mixture was incubated at room temperature for 30 min to remove SMA.[47] The supernatant was obtained after centrifugation at 17000 ×*g* for 3 min. Then, 5 mg of *E. coli* polar lipid, 50 μg of MK-7, and 15 μg of $MgCl_2$-treated *Listeria* NDH-2a sample were extruded into 1 mL of 20 mM MOPS–KOH buffer (pH 7.4, containing 30 mM K_2SO_4) for reconstitution of *Listeria* NDH-2a in proteoliposome.

Establishing a tethered bilayer lipid membrane containing *C. thermarum* NDH-2 and *Listeria* NDH-2a

The electrochemical set-up is described elsewhere.[35] An Autolab (Eco-chemie) electrochemical analyzer equipped with a PGSTAT128N potentiostat, SCAN250 module, and FRA32M frequency analyzer was employed for electrochemical measurements with a Ag/AgCl (sat. KCl) reference electrode from Radiometer. All potentials are quoted versus the standard hydrogen electrode (SHE, $E_{SHE} = E_{Ag/AgCl} + 0.199$ V). The electrochemical cell was housed in a Faraday cage to minimize noise. Oxygen-free argon gas was bubbled into the cell solution at the constant flow rate. The cell solution was constantly mixed using a stir bar during cyclic voltammetry experiments to reduce mass diffusion effects of NADH. All impedance spectra were measured at 0.199 V vs SHE.

The SAM and tethered bilayer lipid membrane (tBLM) were assembled as described previously.[35] A SAM consisting of 45%–60% EO_3-cholesterol and 55%–40% 6-mercapto-1-hexanol was used in this study and the composition of the SAM was checked with impedance spectroscopy before each experiment, as described.[35] A 1.78-mL aliquot of 20 mM MOPS–KOH buffer (pH 7.4, containing 30 mM K_2SO_4) was added to the cell, and 200 μL of proteoliposomes containing either *C. thermarum* NDH-2 or *Listeria* NDH-2a was applied in the presence of 10 mM $CaCl_2$. We note that *C. thermarum* NDH-2 could be directly immobilized on a tBLM by adding a purified NDH-2 sample to the electrochemical cell; however, we discovered the quantity of immobilized *C. thermarum* NDH-2 varied largely between experiments with this latter method and hence preparing proteioliposomes prior to tBLM formation was preferred. Formation of the tBLM was verified by monitoring the decrease in double-layer capacitance using an electrochemical impedance spectroscopy.[35] After preparing the tBLM, the cell was first washed with 1 mM EDTA and then thoroughly washed with 20 mM MOPS–KOH buffer pH 7.4, containing 30 mM K_2SO_4. The integrity of the tBLM–SAM system was checked after washing and throughout the experiments by electrochemical impedance spectroscopy.

Electrochemical NDH-2 assay.

All electrochemical experiments were performed with 2 mL of 20 mM MOPS–KOH buffer pH 7.4, containing 30 mM K_2SO_4 in the cell. The experiments were performed at 20 °C in either duplicate or triplicate. For the NADH oxidation assay, cyclic voltammograms were recorded between −0.401 and 0.449 V at a scan rate of 10 mV s^{-1}. MK-7 reduction and oxidation peaks were typically observed at around −0.30 and 0.15 V, respectively. *Escherichia coli* polar lipid extract contains a trace amount of UQ-8, which gave reduction and oxidation peaks at around

−0.10 and 0.35 V, respectively. Using UQ-10, cyclic voltammograms were recorded between −0.201 and 0.599 V at a scan rate of 10 mV s^{-1}. A molar concentration of membrane-incorporated MK-7 was estimated after integrating the MK-7 oxidation peak area to calculate the surface coverage (pmol cm^{-2}),[48] which was divided by the thickness of lipid membrane (4nm). For the NADH and NADPH titration experiments, the MK-7 concentration was fixed at 3-7 mM, and for the MK-7 titration experiments, the NADH concentration was fixed at 200 μM. For the 2-heptyl-4-hydroxyquinoline-*N*-oxide and phenothiazine inhibitory assay, the NADH and MK-7/UQ-10 concentrations were fixed at 200 μM and 3-7 mM, respectively. 2 and 10 mM stocks of inhibitors were prepared in dimethyl sulfoxide (HQNO) or in water (phenothiazines). After formation of the tBLM–SAM system containing NDH-2, these stock solutions were titrated to the solution in the electrochemical cells at end concentrations indicated in the Results section.

Fluorescent liposome assay.

Fluorescent liposome assays were performed in 20 mM MOPS–KOH buffer (pH 7.4, containing 30 mM K_2SO_4) at 20 °C. First, HPTS was encapsulated inside the liposome lumen by rehydrating 5 mg of *E. coli* polar lipid extract in 0.5 mL of MOPS-KOH buffer containing 5 mM HPTS and extruding the lipid suspension through 400-nm nucleopore track-etched membranes. Non-encapsulated HPTS was removed by size-exclusion chromatography in MOPS-KOH buffer using a Nap-5 G25 column (GE Healthcare) according to the manufacturer's instructions. The liposomes with encapsulated HPTS were diluted to about 40 μg mL^{-1} lipid in a cuvette and the ratiometric fluorescence was monitored in real-time by recording the emission at 510 nm as a ratio of excitations at 405 and 455 nm. At specific time points, the extravesicular pH was lowered by addition of a small amount of 1 M HCl, followed by addition of either 4 μM gramicidin or 100 μM CPZ (end concentrations). A calibration curve (ratiometric fluorescence vs known pH) of HPTS in MOPS-KOH buffer was used to convert the ratiometric fluorescence data to lumen pH values.

Supporting Information

Supplementary Figures S1-S3

Acknowledgements

This work was funded by Marsden Fast-Start grant (grant number 16-UOO-185 to Y.N.), the Maurice Wilkins Centre for Molecular Biodiscovery, and The Biotechnology and Biological

Sciences Research Council (grant number BB/R020140/1 to L.J.C.J.). We thank Gabrielle David, PhD, for editing a draft of this manuscript and Huijie Zhang, PhD, for providing some of the template-stripped gold substrates.

Competing Financial Interests

The authors declare no competing financial interests.

References

(1) Hirst, J. Mitochondrial Complex I. *Annu. Rev. Biochem.* **2013**, *82* (1), 551-575.

(2) Steuber, J.; Vohl, G.; Casutt, M. S.; Vorburger, T.; Diederichs, K.; Fritz, G. Structure of the *V. cholerae* Na^+-pumping NADH:quinone Oxidoreductase. *Nature* **2014**, *516* (7529), 62-67.

(3) Kerscher, S.; Dröse, S.; Zickermann, V.; Brandt, U. The Three Families of Respiratory NADH Dehydrogenases. *Results Probl Cell Differ* **2008**, *45* (Chapter 28), 185-222.

(4) Melo, A. M. P.; Bandeiras, T. M.; Teixeira, M. New Insights into Type II NAD(P)H:quinone Oxidoreductases. *Microbiol. Mol. Biol. Rev.* **2004**, *68* (4), 603-616.

(5) Feng, Y.; Li, W.; Li, J.; Wang, J.; Ge, J.; Xu, D.; Liu, Y.; Wu, K.; Zeng, Q.; Wu, J.-W.; Tian, C.; Zhou, B.; Yang, M. Structural Insight into the Type-II mitochondrial NADH Dehydrogenases. *Nature* **2012**, *491* (7424), 478-482.

(6) Heikal, A.; Nakatani, Y.; Dunn, E.; Weimar, M. R.; Day, C. L.; Baker, E. N.; Lott, J. S.; Sazanov, L. A.; Cook, G. M. Structure of the Bacterial Type II NADH Dehydrogenase: A Monotopic Membrane Protein with an Essential Role in Energy Generation. *Mol. Microbiol.* **2014**, *91* (5), 950-964.

(7) Iwata, M.; Lee, Y.; Yamashita, T.; Yagi, T.; Iwata, S.; Cameron, A. D.; Maher, M. J. The Structure of the Yeast NADH Dehydrogenase (Ndi1) Reveals Overlapping Binding Sites for Water- and Lipid-soluble Substrates. *Proc. Natl. Acad. Sci. U.S.A.* **2012**, *109* (38), 15247-15252.

(8) Blaza, J. N.; Bridges, H. R.; Aragão, D.; Dunn, E. A.; Heikal, A.; Cook, G. M.; Nakatani, Y.; Hirst, J. The Mechanism of Catalysis by Type-II NADH:quinone Oxidoreductases. *Sci. Rep.* **2017**, *7*, 40165.

(9) Biagini, G. A.; Viriyavejakul, P.; O'Neill, P. M.; Bray, P. G.; Ward, S. A. Functional Characterization and Target Validation of Alternative Complex I of *Plasmodium falciparum* Mitochondria. *Antimicrob. Agents Chemother.* **2006**, *50* (5), 1841-1851.

(10) Fang, J.: Beattie, D. S. Rotenone-insensitive NADH Dehydrogenase is a Potential Source of Superoxide in Procyclic *Trypanosoma brucei* Mitochondria. *Mol. Biochem. Parasitol.* **2002**, *123* (2), 135-142.

(11) Weinstein, E. A.; Yano, T.; Li, L.-S.; Avarbock, D.; Avarbock, A.; Helm, D.; McColm, A. A.; Duncan, K.; Lonsdale, J. T.; Rubin, H. Inhibitors of Type II NADH:menaquinone Oxidoreductase Represent a Class of Antitubercular Drugs. *Proc. Natl. Acad. Sci. U.S.A.* **2005**, *102* (12), 4548-4553.

(12) Vries, S.; Grivell, L. A. Purification and Characterization of a Rotenone-insensitive NADH:Q6 Oxidoreductase from Mitochondria of *Saccharomyces cerevisiae. FEBS J.* **1988**, *176* (2), 377-384.

(13) Sena, F. V.; Batista, A. P.; Catarino, T.; Brito, J. A.; Archer, M.; Viertler, M.; Madl, T.; Cabrita, E. J.; Pereira, M. M. Type-II NADH:quinone Oxidoreductase from *Staphylococcus aureus* Has Two Distinct Binding Sites and Is Rate Limited by Quinone Reduction. *Mol. Microbiol.* **2015**, *98* (2), 272-289.

(14) Leung, S. C.; Gibbons, P.; Amewu, R.; Nixon, G. L.; Pidathala, C.; Hong, W. D.; Pacorel, B.; Berry, N. G.; Sharma, R.; Stocks, P. A.; Srivastava, A.; Shone, A. E.; Charoensutthivarakul, S.; Taylor, L.; Berger, O.; Mbekeani, A.; Hill, A.; Fisher, N. E.; Warman, A. J.; Biagini, G. A.; Ward, S. A.; O'Neill, P. M. Identification, Design and Biological Evaluation of Heterocyclic Quinolones Targeting *Plasmodium falciparum* Type II NADH:Quinone Oxidoreductase (PfNDH2). *J. Med. Chem.* **2012**, *55* (5), 1844-1857.

(15) Pidathala, C.; Amewu, R.; Pacorel, B.; Nixon, G. L.; Gibbons, P.; Hong, W. D.; Leung, S. C.; Berry, N. G.; Sharma, R.; Stocks, P. A.; Srivastava, A.; Shone, A. E.; Charoensutthivarakul, S.; Taylor, L.; Berger, O.; Mbekeani, A.; Hill, A.; Fisher, N. E.; Warman, A. J.; Biagini, G. A.; Ward, S. A.; O'Neill, P. M. Identification, Design and Biological Evaluation of Bisaryl Quinolones Targeting Plasmodium falciparum Type II NADH:Quinone Oxidoreductase (PfNDH2). *J. Med. Chem.* **2012**, *55* (5), 1831-1843.

(16) Saleh, A.; Friesen, J.; Baumeister, S.; Gross, U.; Bohne, W. Growth Inhibition of *Toxoplasma gondii* and *Plasmodium falciparum* by Nanomolar Concentrations of 1-

Hydroxy-2-Dodecyl-4(1*H*)Quinolone, a High-Affinity Inhibitor of Alternative (Type II) NADH Dehydrogenases. *Antimicrob. Agents Chemother.* **2007**, *51* (4), 1217-1222.

(17) Yamashita, T.; Nakamaru-Ogiso, E.; Miyoshi, H.; Matsuno-Yagi, A.; Yagi, T. Roles of Bound Quinone in the Single Subunit NADH-Quinone Oxidoreductase (Ndi1) from *Saccharomyces cerevisiae. J. Biol. Chem.* **2007**, *282* (9), 6012-6020.

(18) Eschemann, A.; Galkin, A.; Oettmeier, W.; Brandt, U.; Kerscher, S. HDQ (1-Hydroxy-2-dodecyl-4(1*H*)quinolone), a High Affinity Inhibitor for Mitochondrial Alternative NADH Dehydrogenase. *J. Biol. Chem.* **2005**, *280* (5), 3138-3142.

(19) Lin, S. S.; Gross, U.; Bohne, W. Type II NADH Dehydrogenase Inhibitor 1-Hydroxy-2-Dodecyl-4(1*H*)Quinolone Leads to Collapse of Mitochondrial Inner-Membrane Potential and ATP Depletion in *Toxoplasma gondii. Eukaryotic Cell* **2009**, *8* (6), 877-887.

(20) Lin, S. S.; Kerscher, S.; Saleh, A.; Brandt, U.; Gross, U.; Bohne, W. The *Toxoplasma gondii* Type-II NADH Dehydrogenase TgNDH2-I Is Inhibited by 1-Hydroxy-2-Alkyl-4(1H)Quinolones. *Biochim. Biophys. Acta* **2008**, *1777* (11), 1455-1462.

(21) Mogi, T.; MATSUSHITA, K.; Murase, Y.; Kawahara, K.; Miyoshi, H.; Ui, H.; Shiomi, K.; Ōmura, S.; Kita, K. Identification of New Inhibitors for Alternative NADH Dehydrogenase (NDH-II). *FEMS Microbiol. Lett.* **2009**, *291* (2), 157-161.

(22) Yano, T.; Li, L.-S.; Weinstein, E.; Teh, J.-S.; Rubin, H. Steady-state Kinetics and Inhibitory Action of Antitubercular Phenothiazines on *Mycobacterium tuberculosis* Type-II NADH-Menaquinone Oxidoreductase (NDH-2). *J. Biol. Chem.* **2006**, *281* (17), 11456-11463.

(23) Schurig-Briccio, L. A.; Yano, T.; Rubin, H.; Gennis, R. B. Characterization of the Type 2 NADH:Menaquinone Oxidoreductases from *Staphylococcus aureus* and the Bactericidal Action of Phenothiazines. *Biochim. Biophys. Acta* **2014**, *1837* (7), 954-963.

(24) Mogi, T.; Murase, Y.; Mori, M.; Shiomi, K.; Ōmura, S.; Paranagama, M. P.; Kita, K. Polymyxin B Identified as an Inhibitor of Alternative NADH Dehydrogenase and

Malate: Quinone Oxidoreductase from the Gram-positive Bacterium *Mycobacterium smegmatis*. *J Biochem* **2009**, *146* (4), 491-499.

(25) Deris, Z. Z.; Akter, J.; Sivanesan, S.; Roberts, K. D.; Thompson, P. E.; Nation, R. L.; Li, J.; Velkov, T. A Secondary Mode of Action of Polymyxins against Gram-negative Bacteria Involves the Inhibition of NADH-Quinone Oxidoreductase Activity. *J. Antibiot.* **2014**, *67* (2), 147-151.

(26) Petri, J.; Shimaki, Y.; Jiao, W.; Bridges, H. R.; Russell, E. R.; Parker, E. J.; Aragão, D.; Cook, G. M.; Nakatani, Y. Structure of the NDH-2 – HQNO Inhibited Complex Provides Molecular Insight into Quinone-Binding Site Inhibitors. *Biochim. Biophys. Acta, Bioenerg.* **2018**, *1859* (7), 482-490.

(27) Yamashita, T.; Inaoka, D. K.; Shiba, T.; Oohashi, T.; Iwata, S.; Yagi, T.; Kosaka, H.; Miyoshi, H.; Harada, S.; Kita, K.; Hirano, K. Ubiquinone Binding Site of Yeast NADH Dehydrogenase Revealed by Structures Binding Novel Competitive- and Mixed-Type Inhibitors. *Sci. Rep.* **2018**, *8* (1), 2427.

(28) Weinstein, E. A.; Yano, T; Li, L-S.; Avarbock, D.; Avarbock, A; Helm, D.; McColm, A. A.; Duncan, K.; Lonsdale, J. T.; Rubin, H. Inhibitors of Type II NADH:menaquinone Oxidoreductase Represent A Class of Antitubercular Drugs. *Proc. Natl. Acad. Sci. USA* **2005**, *102* (12), 4548-4553.

(29) Griffin, J. E.; Gawronski, J. D.; Dejesus, M. A.; Ioerger, T. R.; Akerley, B. J.; Sassetti, C. M. High-Resolution Phenotypic Profiling Defines Genes Essential for Mycobacterial Growth and Cholesterol Catabolism. *PLoS Pathog.* **2011**, *7* (9), e1002251.

(30) Sassetti, C. M.; Boyd, D. H.; Rubin, E. J. Genes Required for Mycobacterial Growth Defined by High Density Mutagenesis. *Mol. Microbiol.* **2003**, *48* (1), 77-84.

(31) Shirude, P. S.; Paul, B.; Roy Choudhury, N.; Kedari, C.; Bandodkar, B.; Ugarkar, B. G. Quinolinyl Pyrimidines: Potent Inhibitors of NDH-2 as a Novel Class of Anti-TB Agents. *ACS Med Chem Lett* **2012**, *3* (9), 736-740.

(32) Yang, Y.; Yu, Y.; Li, X.; Li, J.; Wu, Y.; Yu, J.; Ge, J.; Huang, Z.; Jiang, L.; Rao, Y.; Yang, M. Target Elucidation by Cocrystal Structures of NADH-Ubiquinone Oxidoreductase of *Plasmodium falciparum* (Pf NDH2) with Small Molecule To Eliminate Drug-Resistant Malaria. *J. Med. Chem.* **2017**, *60* (5), 1994-2006.

(33) Yano, T.; Rahimian, M.; Aneja, K. K.; Schechter, N. M.; Rubin, H.; Scott, C. P. *Mycobacterium tuberculosis* Type II NADH-Menaquinone Oxidoreductase Catalyzes Electron Transfer through a Two-Site Ping- Pong Mechanism and Has Two Quinone-Binding Sites. *Biochemistry* **2014**, *53* (7), 1179-1190.

(34) Lencina, A. M.; Franza, T.; Sullivan, M. J.; Ulett, G. C.; Ipe, D. S.; Gaudu, P.; Gennis, R. B.; Schurig-Briccio, L. A. Type 2 NADH Dehydrogenase Is the Only Point of Entry for Electrons into the *Streptococcus agalactiae* Respiratory Chain and Is a Potential Drug Target. *mBio* **2018**, *9* (4), e01034.

(35) Jeuken, L. J. C.; Connell, S. D.; Henderson, P. J. F.; Gennis, R. B.; Evans, S. D.; Bushby, R. J. Redox Enzymes in Tethered Membranes. *J. Am. Chem. Soc.* **2006**, *128* (5), 1711-1716.

(36) Jeuken, L. J. C.; Daskalakis, N. N.; Han, X.; Sheikh, K.; Erbe, A.; Bushby, R. J.; Evans, S. D. Phase Separation in Mixed Self-assembled Monolayers and Its Effect on Biomimetic Membranes. *Sens. Actuators*, *B* **2007**, *124* (2), 501-509.

(37) Weiss, S. A.; Bushby, R. J.; Evans, S. D.; Henderson, P. J. F.; Jeuken, L. J. C. Characterization of Cytochrome *bo*3 Activity in a Native-Like Surface-Tethered Membrane. *Biochem. J.* **2009**, *417* (2), 555-560.

(38) Jeuken, L. J. C.; Bushby, R. J.; Stephen, D. E.; Proton Transport into a Tethered Bilayer Lipid Membrane. *Electrochemistry Communications* **2007**, 9 (4), 610-614.

(39) Godoy-Hernandez, A.; Tate, D. J.; McMillan, D. G. G. Revealing the Membrane-Bound Catalytic Oxidation of NADH by the Drug Target Type-II NADH Dehydrogenase. *Biochemistry* **2019**, *58* (42), 4272-4275.

(40) Kendall, J. K. R.; Johnson, B. R. G.; Symonds, P. H.; Imperato, G.; Bushby, R. J.; Gwyer, J. D.; van Berkel, C.; Evans, S. D.; Jeuken, L. J. C. Effect of the Structure of

Cholesterol-Based Tethered Bilayer Lipid Membranes on Ionophore Activity. *ChemPhysChem* **2010**, *11* (10), 2191-2198.

(41) WHO Expert Committee. The Selection and Use of Essential Medicines. *World Health Organ. Tech. Rep. Ser*. **2017**, 1-331.

(42) Seeman, P. Dopamine D2 Receptors as Treatment Targets in Schizophrenia. *Clinical Schizophrenia & Related Psychoses* 2010, *4* (1), 56-73.

(43) Light, S. H.; Su, L.; Rivera-Lugo, R.; Cornejo, J. A.; Louie, A.; Iavarone, A. T.; Ajo-Franklin, C. M.; Portnoy, D. A. A Flavin-Based Extracellular Electron Transfer Mechanism in Diverse Gram-positive Bacteria. *Nature* **2018**, *562* (7725), 140-144.

(44) Lee, S. C.; Knowles, T. J.; Postis, V. L. G.; Jamshad, M.; Parslow, R. A.; Lin, Y.-P.; Goldman, A.; Sridhar, P.; Overduin, M.; Muench, S. P.; Dafforn, T. R. A Method for Detergent-Free Isolation of Membrane Proteins in Their Local Lipid Environment. *Nat. Protocols* **2016**, *11* (7), 1149-1162.

(45) Nakatani, Y.; Jiao, W.; Aragão, D.; Shimaki, Y.; Petri, J.; Parker, E. J.; Cook, G. M. Crystal Structure of Type II NADH:quinone Oxidoreductase from *Caldalkalibacillus thermarum* with an Improved Resolution of 2.15 Å. *Acta Crystallogr. Sect. F: Struct Biol Commun* **2017**, *73* (Pt 10), 541-549.

(46) Miroux, B.; Walker, J. E. Over-production of Proteins in Escherichia coli: Mutant Hosts that Allow Synthesis of some Membrane Proteins and Globular Proteins at High Levels. *J. Mol. Biol.* **1996**, *260* (3), 289-298.

(47) Smirnova, I. A.; Ädelroth, P.; Brzezinski, P. Extraction and Liposome Reconstitution of Membrane Proteins with Their Native Lipids without the Use of Detergents. *Sci. Rep.* **2018**, *8* (1), 14950.

(48) Armstrong, F. A.; Heering, H. A.; Hirst, J. Reaction of Complex Metalloproteins Studied by Protein-Film Voltammetry. *Chem. Soc. Rev.* **1997**, *26* (3), 169-179.

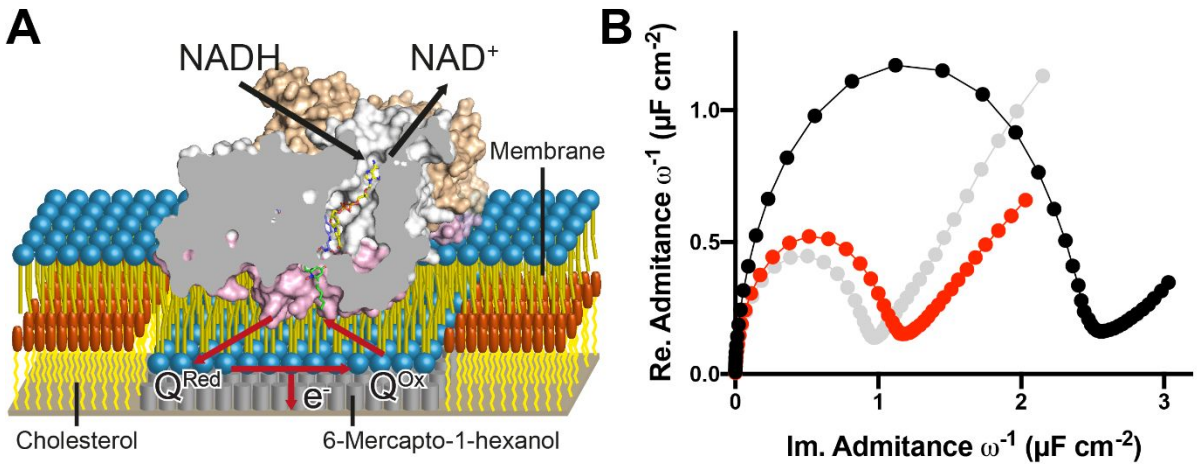

Figure 1. New bioelectrochemical platform for analysis of the monotopic membrane protein NDH-2 in the membrane environment. (A) Schematic diagram of *C. thermarum* NDH-2 bound on the tethered bilayer lipid membrane, which is self-immobilized on a self-assembled monolayer made of a mixture of 6-mercapto-1-hexanol and a cholesterol 'tether' (a cholesterol linked to a thiol group via a short ethylene-glycol chain). NDH-2 oxidizes NADH in the aqueous phase, while quinone is reduced and re-oxidized in the lipid phase on the gold surface. Molecules of NAD^+, FAD, and the quinone are shown in yellow, purple, and green, respectively. (B) Cole–Cole plots of real (Re) and imaginary (Im) admittances before (black) and after (red) applying proteoliposomes containing *C. thermarum* NDH-2. A drop in capacitance indicates formation of planar membrane. Another Cole–Cole plot checking membrane after the experiments in Figure 2A is shown in grey.

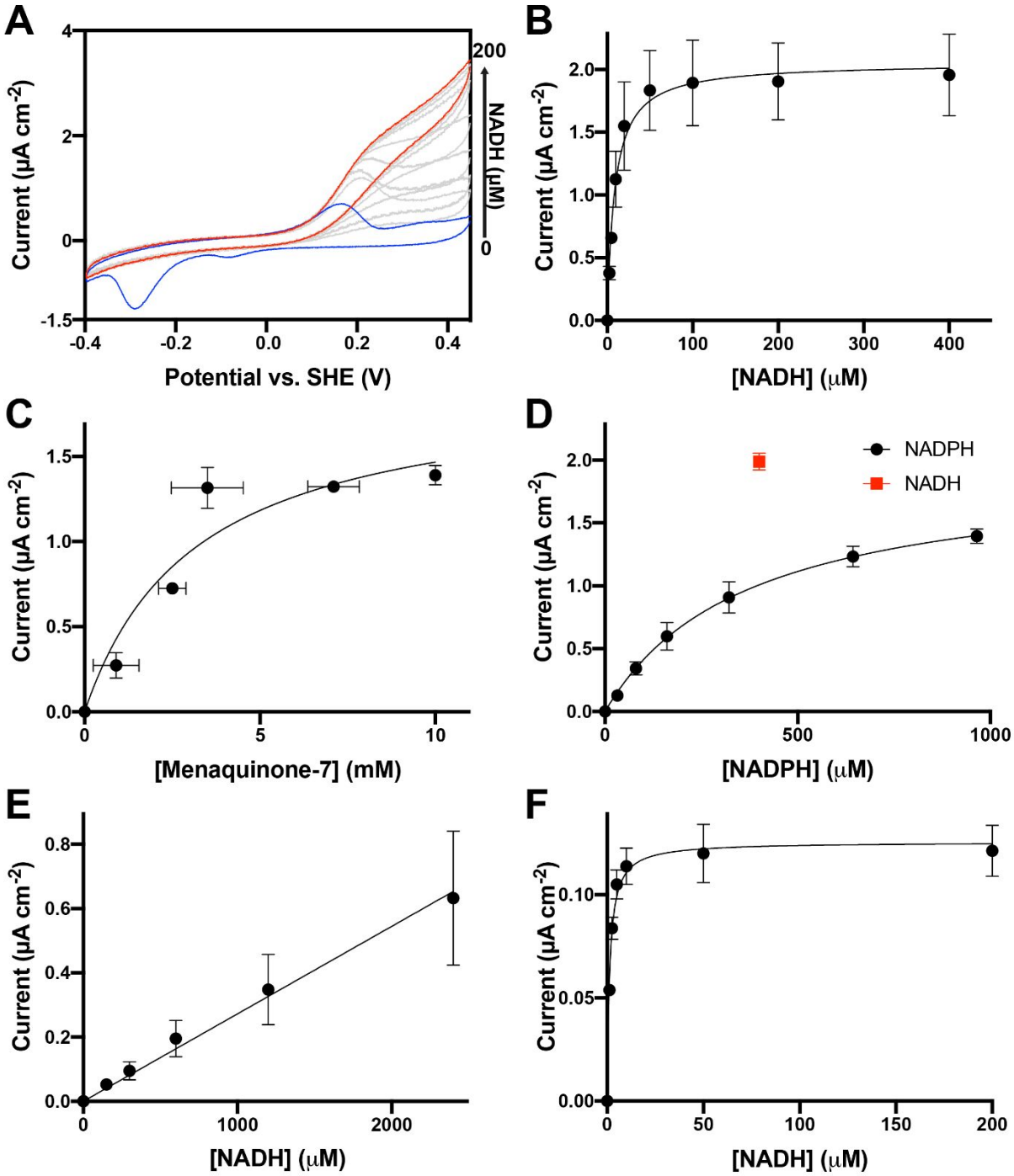

Figure 2. Steady-state electrochemical enzyme kinetics of *C. thermarum* NDH-2 bound on membrane. (A) Cyclic voltammogrames (CVs) recorded at various NADH concentrations (0 (blue)–400 (red) μM) for a wild-type NDH-2. Currents read at 0.3 V versus the standard hydrogen electrode (SHE) of the reductive scan were used in panel B. (B), (C), and (D) NADH, MK-7, and NADPH titration experiments for wild-type NDH-2, respectively. After the NADPH titration experiment, the electrochemical cell was washed and NADH was added to measure the activity (red). (E) and (F) NADH titration experiments for G164E and I379E

NDH-2 variants, respectively. The data were fitted to the Michealis–Menten equation, except for data in panel E. The data points and error bars are averages ± SEM from two or three technical replicates.

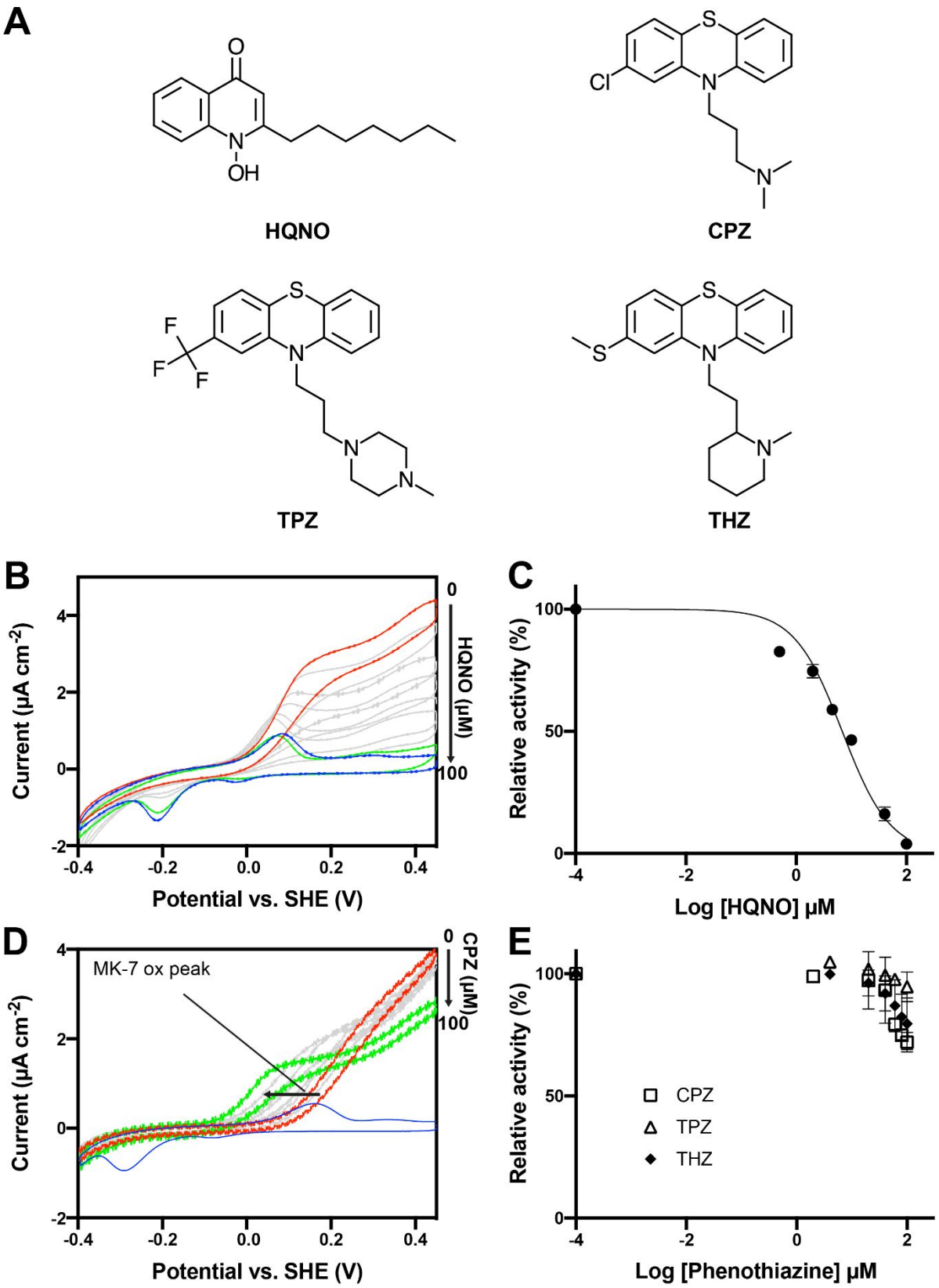

Figure 3. Electrochemical assays showing HQNO inhibits *C. thermarum* NDH-2 but phenothiazines do not. (A) Chemical structures of HQNO and phenothiazines tested in this study. (B) CVs recorded in the presence of 0 (red)–100 (green) μM HQNO. Other HQNO

concentrations are shown in grey. A baseline CV (blue) in the absence of both NADH and HQNO is also shown. (C) HQNO inhibition curve. The *C. thermarum* NDH-2 activity in the absence of HQNO was taken as 100%. A variable slope model was fitted to determine the IC_{50} value. (D) CVs recorded for CPZ experiments. CVs were recorded in the presence of 0 (red)–100 (green) μM CPZ. The MK-7 oxidation peak shift is shown with an arrow. (E) Phenothiazines do not inhibit *C. thermarum* NDH-2. The NDH-2 activity in the absence of phenothiazines was taken as 100%. All experiments were performed in the presence of 200 μM NADH and 3-7 mM MK-7, and in duplicate.

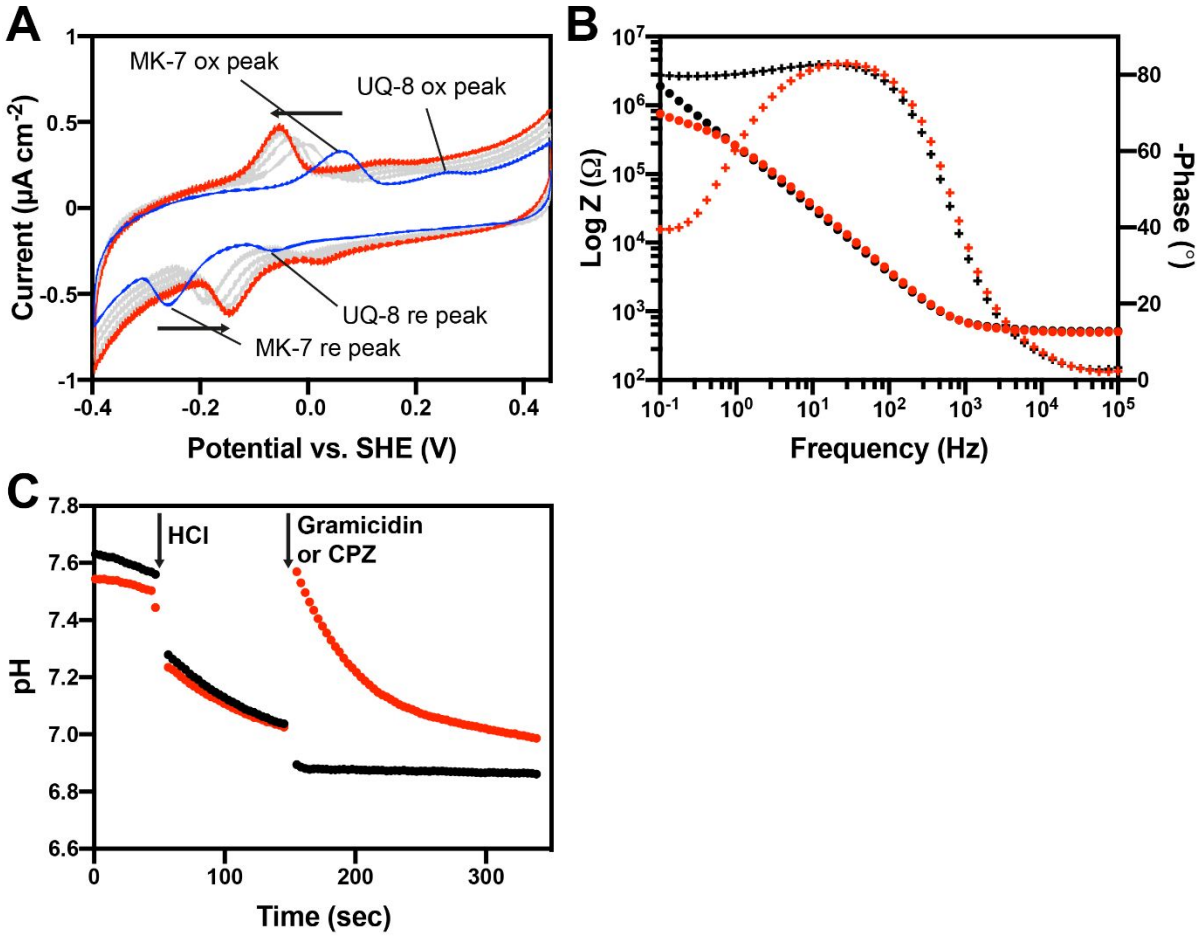

Figure 4. Ionophore effects of CPZ. (A) CVs recorded with 0 (blue), 10, 30, 60, and 100 (red) μM CPZ in the absence of NADH show clear shifts of MK-7 oxidation (ox) and reduction (re) peaks. *Escherichia coli* polar lipid extract contained a small amount of UQ-8. Shifts of UQ-8 ox and re peaks are also evident. (B) Bode plots (+) and impedance (circles) before (black) and after (red) addition of 100 μM CPZ. (C) Fluorescent liposome assays using 8-hydroxypyrene-1,3,6-trisulfonic acid as a pH probe. Points of addition of 1 M HCl and ionophores are indicated with arrows. Experiments were conducted with gramicidin (black) and CPZ (red).

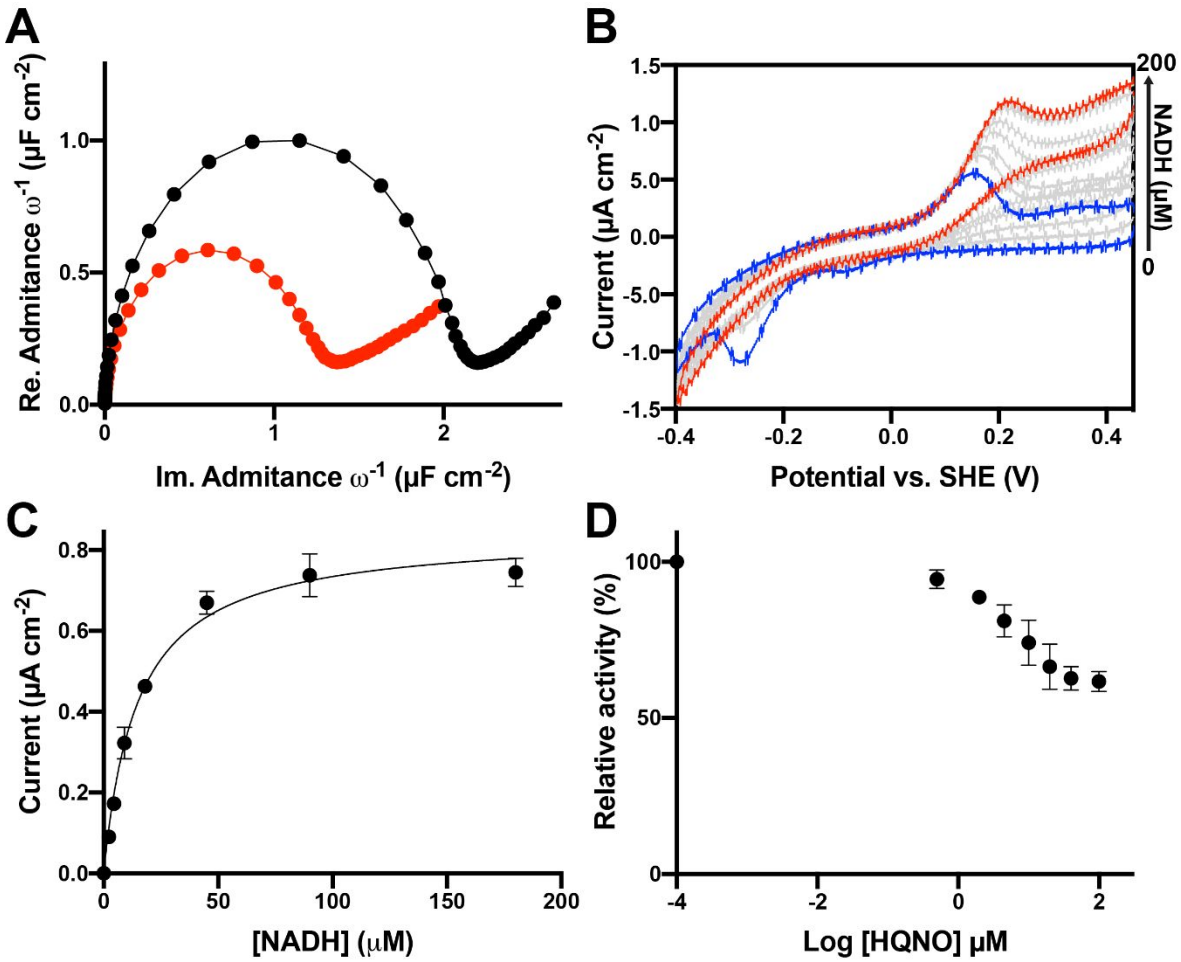

Figure 5. Characterization of *Listeria* NDH-2a using the electrochemical NDH-2 assay platform. (A) Cole–Cole plots measured at 0 V versus the SCE before (black) and after (red) applying a proteoliposome containing *Listeria* NDH-2a. (B) CVs recorded with 0 (blue)–180 (red) μM NADH. Currents read at 0.3 V versus the SHE of the reductive scan are used in panel C. (C) Steady-state kinetic analysis of *Listeria* NDH-2a. The data were fit to the Michealis–Menten equation. (D) HQNO does not inhibit *Listeria* NDH-2a efficiently. The *Listeria* NDH-2 activity in the absence of HQNO was taken as 100%. All experiments were performed in the presence 3-7 mM MK-7. The data points and error bars are averages ± SEM from two or three technical replicates.

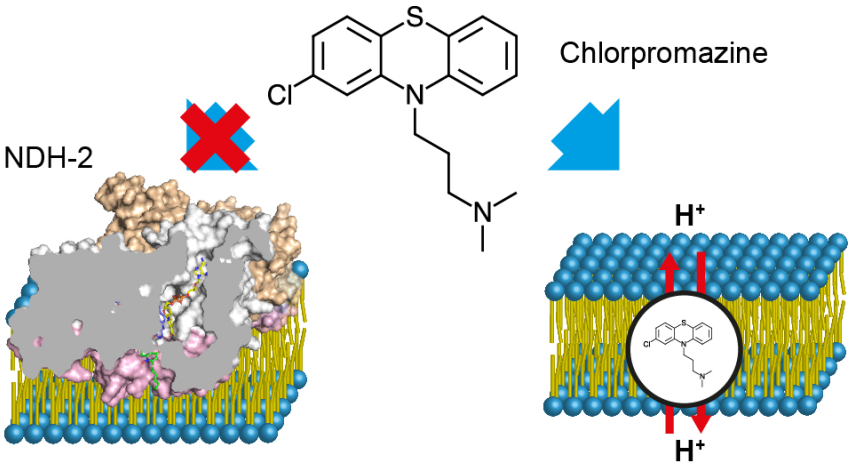

TOC